https://doi.org/10.46813/2024-149-176

UDC 621.793: 539.21

EFFECT OF PULSED SUBSTRATE BIAS ON THE STRUCTURE AND PROPERTIES OF NITRIDE COATINGS DEPOSITED BY FILTERED CATHODIC ARC PLASMA

E.N. Reshetnyak, V.E. Strel'nitskij, V.V. Vasyliev, A.A. Luchaninov
National Science Center "Kharkov Institute of Physics and Technology", Kharkiv, Ukraine
E-mail: reshetnyak@kipt.kharkov.ua

The results of studies of nitride coatings deposited using a cathodic vacuum arc plasma source with a rectilinear type filter are presented. The effect of parameters of high voltage substrate bias pulses on the deposition rate, composition, structure and mechanical properties of coatings based on TiN and CrN, including multi-component ones with the additions of Al, Si, Zr, Y, Re, Nb, Hf, was analyzed. With different regimes of bias potential the formation of coatings with a nanocrystalline cubic structure (of the NaCl type) and close to stoichiometric nitrogen content and high hardness of 25…36 GPa is ensured. It was found that changing the amplitude, duration and frequency of pulses allows to effectively controlling the morphology, size of crystallites, texture and stress level in coatings, which effects their mechanical properties. The use of a pulse bias potential with an amplitude of 1…2 kV, a frequency of 10…20 kHz and duty cycle of 10…15% makes it possible to form a homogeneous dense nanostructure with a [110] or [100] texture, an optimal stress level 4…5 GPa and a smooth surface in coatings of different compositions. It is shown that such a structure provides improved resistance of coatings to various types of wear. Unequivocal correlations were not found between the hardness of the coatings, the modulus of elasticity and their wear.

INTRODUCTION

The cathodic vacuum-arc deposition process is widely used in industry for the synthesis of wear-resistant coatings based on transition metal nitrides on the surface of tools and machine parts. The advantages of the method include a high deposition rate, good adhesion, and a wide range of applicable reaction gas pressures. Targeted formation of nanostructure coatings can create materials with a fundamentally new set of physicochemical properties and expand the scope of application of cathodic arc technology in various industries [1–3]. Among nanostructured coatings for surface strengthening, multicomponent coatings based on a combination of nitrides with metallic (TiN, CrN, ZrN, etc.) and covalent (Si_3N_4, AlN, BN) types of bonds are considered the most promising. The limited solubility of components in such systems makes it possible to form structures consisting of nanocrystalline grains interconnected by strong thin amorphous layers under non-equilibrium deposition conditions. The latest trends in the development of new protective coatings are attempts to combine the best properties of various systems by increasing the number of components, for example, adding metals (Y, Re, Nb, Hf, Ni, V, Mo) to their composition, which can improve the resistance of coatings to oxidation and wear [4–6].

Controlling the energy of the particles that form the coating is a key lever of influence on the composition, growth mechanisms, microstructure, morphology, defects and stresses in the coatings, and therefore on their functional properties [7, 8]. The plasma generated by the cathodic arc is highly ionized and contains a high concentration of metal ions whose energy can be effectively changed by applying a bias potential to the substrate [1–3]. A promising technique used in the synthesis of multifunctional coatings is the combination of the condensation process with ion implantation, which is carried out by applying a high-voltage pulse bias potential to the substrate. Intense ion bombardment during coating deposition makes it possible to synthesize a coating with a dense nanocrystalline structure, reduced stress level and improved adhesion at low substrate temperatures [9–11].

A feature of the arc discharge is the presence in the plasma flow the drops of cathode material – macroparticles, which, falling into the coating, disrupt its uniformity and lead to a decrease in hardness, an increase in surface roughness, and a deterioration in adhesion. Magnetoelectric filters of various geometries have been developed to separate the ionic component of the plasma flow, which is purified from the droplet component. Previously, filters were not widely used for the synthesis of nitride coatings due to low productivity [1, 12]. Now it is clear that the creation of high-quality nanostructured coatings is impossible in the presence of defects in the form of micrometer-sized drops. A new high-performance source of cathodic arc plasma equipped with a rectilinear filter with a magnetic island was created at the National Science Center "Kharkov Institute of Physics and Technology" (NSC KIPT). The main advantages of this source: high deposition rate; stability of parameters regardless of the degree of cathode burnout; ensuring the uniformity of the coating thickness over a large area with high-quality plasma cleaning from macroparticles; structural simplicity, low manufacturing cost compared to well-known sources with curvilinear filters [13]. In this work, we summarize the results of research devoted to the complex application of a rectilinear plasma source and a high-voltage pulsed bias potential on a substrate for the synthesis of nanostructured coatings based on transition metal nitrides, conducted during the last decade. The main goal of the work is the analysis of the influence of

the parameters of high voltage substrate bias pulses on the on the structure and properties of coatings based on TiN and CrN, including multi-component ones with the addition of Al, Si, Zr, Y, Re, Nb, Hf.

1. EXPERIMENTAL DETAILS

The coating was deposited by the cathodic vacuum-arc method on a modernized installation of the Bulat-6 type, which is equipped with a rectilinear magnetoelectric plasma filter against macroparticles [13]. For the coatings synthesis, cathodes made of technically pure Ti, $Ti_{0.6}Cr_{0.4}$ and $Ti_{0.5}Al_{0.5}$ alloys, including those with the addition of a small amount (up to 2 at.%) of Y and Re, alloy $Ti_{0.48}Zr_{0.18}Al_{0.18}Nb_{0.09}Y_{0.07}$. $Ti_{0.85}Si_{0.15}$ and $Cr_{0.5}Al_{0.5}$ cathodes made by the powder metallurgy method were also used. Nitrogen pressure in the vacuum chamber within the range of 0.05…0.1 Pa was chosen in such a way that the concentration of nitrogen in the coatings was about 50 at.%. The arc discharge current was 100 A.

Coatings deposition with a thickness of 5…10 μm was carried out on steel substrates under the conditions of applying a negative high-voltage pulse bias potential. The characteristics of the potential pulses varied within: amplitude (U) 500…2500 V, duration (t_p) 5…20 μs, repetition frequency (f) 1.3…24 kHz. In the intervals between pulses, the substrate was at a self-consistent "floating" potential 3…20 V. The substrate temperature during the coating deposition process was not forcibly regulated and changed due to radiation-stimulated heating. The coating surface temperature during deposition was measured using an infrared pyrometer "Raynger MX4". When using pulsed potential, radiation heating of the surface did not exceed 300 °C.

Titanium nitride (TiN) is one of the first and still common materials for creating wear-resistant cathodic arc coatings. Currently, research interest in the field of hard coatings is shifted towards the synthesis of multicomponent coatings based on various transition metal nitrides, however, TiN remains an excellent test object for the development of new coating synthesis processes [14, 15]. That is why, in our studies of processes of reactive deposition of coatings from filtered plasma of metal cathodes, considerable attention was paid to TiN. In order to study the influence of pulse potential parameters on the structure and properties of coatings, several series of samples with TiN coatings were synthesized. The samples of the first series were deposited at fixed values of duration t_p = 5 μs and frequency f = 24 kHz and different amplitudes of the pulse potential ranging from 0 kV, when the deposition occurs at a floating substrate potential, to 2.5 kV. The plasma ion flow density on the substrate, which determines the coating deposition rate, was regulated by changing the distance between the plasma source and the substrate within 180…350 mm. During the deposition of the second series of TiN samples, the time parameters of the potential pulses t_p and f were changed at a fixed amplitude U = 1.5 kV. The potential parameters used in the synthesis of multicomponent coatings are listed in Table 1.

The morphology and elemental composition of the coatings surface, as well as their transverse fractures, were studied on a JEOL 7100F scanning electron microscope with an X-ray spectral energy dispersive microanalysis system. The relief and surface roughness of the coatings (R_a) were studied using a Dimension 3000 NanoScopeIIIa scanning atomic force microscope. Microscopic images of the surface of coated samples in the initial state and after adhesion, cavitation, and tribological tests were studied using an electron microscope or a Leica MTU 253 optical microscope. The phase composition, texture, substructure, and stresses in the coatings were studied by X-ray structural analysis using Philips PW3710 diffractometers and DRON-3 in Cu-Kα radiation. The size of the crystallites (L) (coherent scattering zone) was calculated from the broadening of the diffraction peaks from the Scherrer ratio. The study of texture in coatings was carried out by calculating texture coefficients:

$$T_C = \left[nI_m^{(hkl)} / I_0^{(hkl)} \right] / \left[\sum I_m^{(hkl)} / I_0^{(hkl)} \right],$$

where $I_m^{(hkl)}$ is the measured integral reflection intensity (hkl); $I_0^{(hkl)}$ – relative reflection intensity (hkl) for powder non-textured material; n is the number of reflections [16]. The level of residual stresses (σ) was determined by X-ray tensometry using the $sin^2\psi$ method adapted for textured samples [14, 17, 18].

The hardness (H) and Young's modulus (E) of the coatings were measured by a G200 nanoindenter manufactured by MTS using the CSM (continuous hardness measurement) method. Adhesion of coatings to the substrate was evaluated based on the results of scratch tests on the CSM Instruments REVETEST device with a Rockwell indenter. Tribological tests of the coatings were carried out on an installation with a reciprocating testing system, a counterbody made of a corundum ball with a diameter of 10 mm under a load of 5 N, a speed of movement of 1 cm/s and a full distance of 100 m. Erosion resistance was assessed by the gravimetric method based on the results of cavitation tests in distilled water at room temperature on an installation with a magneto-striction vibrator MSV-1 at a frequency of 20 kHz and an amplitude of (30 ± 2) μm. The tests continued until the formation of through defects in the coating. Abrasive wear was determined by the plane-disc scheme. The speed of movement of the surface of the abrasive disk (with corundum abrasive particles) in contact with the surface of the sample was 4.4 m/s, the load on the sample was 2.2 N.

2. RESULTS AND DISCUSSION

2.1. DEPOSITION RATE, MORPHOLOGY AND ELEMENTAL COMPOSITION OF COATINGS

In Fig. 1 shows the deposition rate of TiN, TiAlYN, CrAlN, CrTiN, and TiZrAlNbYN coatings obtained using filtered plasma at different parameters of the pulse bias potential on the substrate. In Fig. 1,a and b shows the dependence of the deposition rate on the pulse amplitude U, and Fig. 1,c – on the duty cycle, which is numerically equal to the product of their frequency and duration ($f \cdot t_p \cdot 100\%$). The coefficient shows the percentage relationship between the duration of the

pulses and their period, that is, the percentage that constitutes the time of action of the high-voltage potential from the total time of deposition. It can be seen that when the amplitude increases in the range of 0…2.5 kV or the duty cycle in the range of 1.3…24%, the deposition rate tends to decrease, however, the change is not significant enough – no more than 10%.

Table 1

Potential parameters during deposition, structural characteristics and results of nanoindentation of multicomponent coatings

N	Potential parameters					R_a, nm	Texture axis	a, nm	L, nm	H, GPa	E, GPa	H/E
	U, kV	f, kHz	t_p, μs	$f{\cdot}t_p$,%	$U{\cdot}f{\cdot}t_p$, V							
Cathode composition – $Ti_{0.5}Al_{0.5}$												
1	1.5	24	5	12	180	80	[110]	0.4212	13	29.5	404	0.07
Cathode composition – $Ti_{0.49}Al_{0.5}Y_{0.01}$												
2	0	24	5	12.0	0		[111]	0.4204	21	36.0	445	0.08
3	0.5				60	10	[110]	0.4194	9	34.1	408	0.08
4	1.0				120	15	[110]	0.4191	13	32.6	350	0.09
5	1.5				180	15	[110]	0.4195	9	35.8	418	0.09
6	2.5				300	17	[110]+ [100]	0.4209	7	25.1	300	0.08
Cathode composition – $Ti_{0.49}Al_{0.50}Y_{0.009}Re_{0.001}$												
7	1.5	24	5	12.0	180		[100]	0.4225	6	28.2	354	0.08
Cathode composition – $Cr_{0.5}Al_{0.5}$												
8	0	12	12	14.5	0	38	[111]	0.4166	18	29.6	404	0.07
9	0.5				72	36	[110]	0.4186	9	33.4	390	0.09
10	1.0				144	56	[110]	0.4190	7	33.1	385	0.09
11	1.5				216	45	[110]	0.4185	6	36.2	436	0.08
12	2.0				288	50	[110]+ [100]	0.4168	6	30.5	385	0.08
13	2.5				360	52	[110]+ [100]	0.4170	7	30.2	373	0.08
Cathode composition – $Ti_{0.48}Zr_{0.18}Al_{0.18}Nb_{0.09}Y_{0.07}$												
14	1.0	1.3	6	0.8	8	19	[100]	0.4371	32	30.8	382	0.08
15		2.5		1.5	15	7	[100]	0.4413	28	29.8	358	0.08
16		12		7.2	72	12	[100]	0.4390	13	29.8	357	0.08
Cathode composition – $Ti_{0.85}Si_{0.15}$												
2	0	12	6	7.2	0		-	0.4245	10	30.0		
3	0.5				36		[110]	0.4251	7	32.1		
4	1.0				72		[110]	0.4250	6	37.1		
5	1.5				108		[110]	0.4249	6	26.4		
6	2.5				180		[110]	0.4243	7	20.3		
Cathode composition – $Ti_{0.6}Cr_{0.4}$												
2	0.5	12	6	7.2	36		[110]	0.4194	11	31.6	359	0.09
3	1.0				72		[110]	0.4223	6	29.0	333	0.09
4	1.5				108		[110]	0.4224	5	29.5	352	0.07

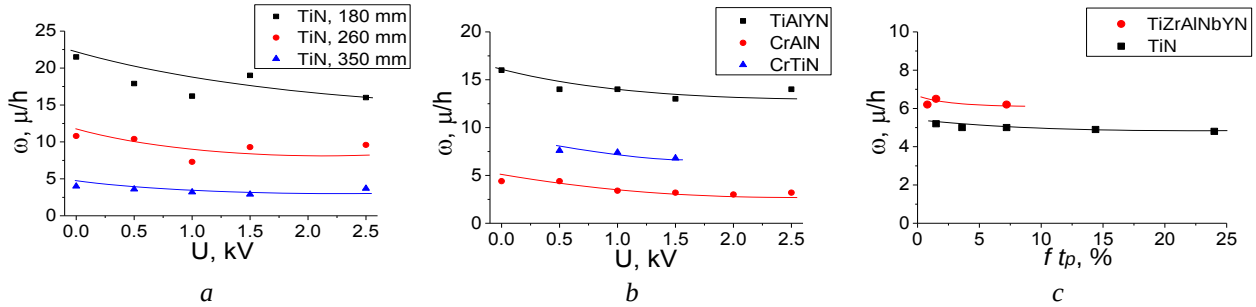

a *b* *c*

Fig. 1. The effect of the amplitude (a, b), the duty cycle (c) and the distance between the filter outlet and the substrate (a) on the coatings deposition rate of different elemental composition

That is, the application of a high pulsed potential does not lead to significant sputtering of the deposition surface bombarded by accelerated plasma ions, in contrast to a constant potential. Thus, during the synthesis of TiN cathodic arc coatings at a constant bias potential on the substrate of about 1.5 kV, the deposition mode changes to the etching one [19, 20]. The location of the sample in the vacuum chamber has a much stronger effect on the deposition rate, which can be seen on the example of TiN coatings. Fig. 1,a shows the dependence of the TiN coatings deposition rate on substrates located at different distances *R* from the filter outlet of 180, 260, or 350 mm. The maximum deposition rate of about 20 μm/h is observed at a distance of 180 mm. When the distance increases, the speed decreases inversely proportional to R^2, up to 5 μm/h, which is due to the divergence and dispersion of the plasma flow.

Microscopic studies of the samples showed that the coatings surface of all systems, thanks to the use of the filter, is smooth, does not contain macroparticles and reproduces the relief of the substrate surface, which indicates a high quality of filtration. Typical electron microscopic cross-sectional images of coated samples are shown in Fig. 2. It can be seen that there are no defects in the form of drops on the surface and in the volume of the coatings. All coatings have a nanocrystalline structure and consist of narrow (≤100 nm) columnar grains. The fracture structure is dense and has a step-like appearance. When varying the parameters of the potential, small changes in the thickness and length of the columnar grains in the coatings were detected while preserving the general appearance of the fracture structure [21]. In particular, at potential pulse amplitude of 0.5 kV, the cross-section of the fracture of the TiN coating (see Fig. 2,a) is similar to the transition region between zone T and zone 2 in the structural zone diagram proposed by Anders [7]. For coatings synthesized using an amplitude of 1…2.5 kV, the structure of transverse fractures (see Fig. 2,b,c) is similar to the structure of zone 2. It can be seen that with increasing amplitude, the structure becomes more dense and uniform, and the width of the columns increases slightly. With an increase in the number of elements in the coatings, the width of the nanostructured columnar grains decreases and the cross-sectional structure of the multicomponent coatings takes on a rather needle-like shape. Columnar growth is interrupted. For example, the narrow columns in the TiAlYN coating (see Fig. 2,c) do not extend from the substrate to the surface as clearly as in the TiN coating deposited under identical conditions (see Fig. 2,b).

In Fig. 3 shows typical atomic force microscopic 3D images of the samples surface [22]. The coatings have a high quality surface with a cellular morphology characteristic of ion-plasma coatings. The rms value of the surface roughness R_a, determined from the 3x3 μm image for TN coatings is in the range of 20…40 nm (see Table 1). For multi-component coatings, the range of R_a values is wider – within 7…80 nm. TiAlN and CrAlN coatings have high roughness. Multicomponent TiZrAlNbYN coatings have a lower surface roughness of 7…18 nm, which changes non-monotonically with increasing frequency of potential pulses. It is interesting that the addition of even 1 at.% Y to the composition of the TiAlN cathode helps to reduce the roughness by up to 5 times. Cell elements that protrude above the plane of the coating have a rounded or pointed shape of different heights depending on the composition of the coating and potential parameters.

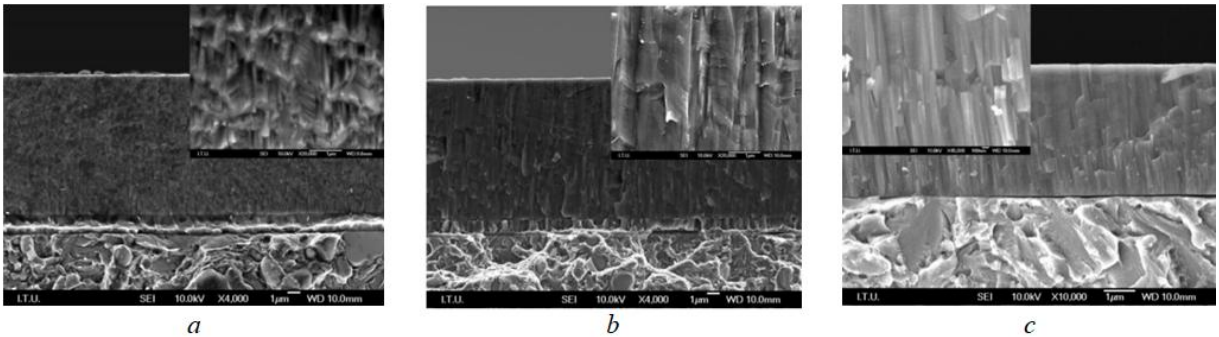

Fig. 2. Electron microscopic images of the cross section of TiN (a, b) and TiAlYN (c) coatings obtained at substrate potential amplitudes of 0.5 kV (a) and 1.5 kV (b, c)

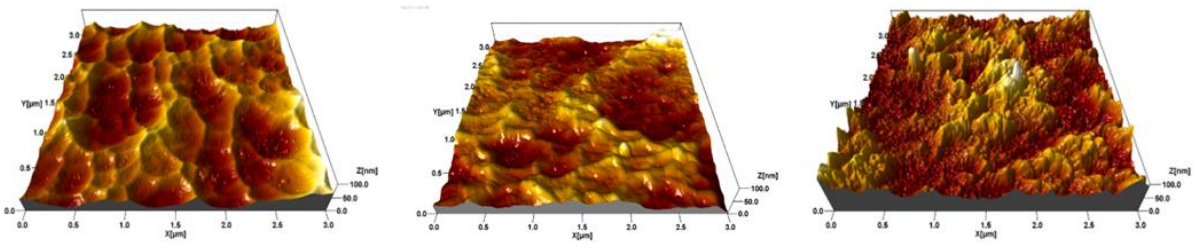

Fig. 3. The influence of the potential amplitude on the surface morphology of TiAlYN coatings (atomic force microscopy): a – 0.5 kV; b – 1.5 kV; c – 2.5 kV

In particular, the surface of the TiAlYN coatings obtained at a potential amplitude of 0.5…1.5 kV has a relief with concave cells of the order of several hundred nanometers and a surface roughness of 10…15 nm (see Fig. 3,a, b). When the amplitude of the pulses increases to 2.5 kV, the surface of the cells is completely covered with small structural elements of nanometer sizes. Due to the more developed relief, the surface roughness of this coating increases to 17 nm. A similar increase in roughness with increasing amplitude is observed for CrAlN.

All coatings obtained using Ti cathodes have a golden color characteristic of titanium nitride. EDS analysis confirms that the elemental composition is close to the stoichiometric composition of TiN mononitride. Similar results regarding the nitrogen content were obtained for multicomponent coatings. Regardless of the parameters of the substrate pulse potential, the concentration of nitrogen in all investigated coatings was about 50 at.%. An important factor in the synthesis of multicomponent systems is the degree of reproducibility of the composition of the cathode in the coating. The analysis of the elemental composition of the coatings showed that when using $Cr_{0.5}Al_{0.5}$ and $Ti_{0.5}Al_{0.5}$cathodes, including with the addition of a small amount (up to 2 at.%) of Y and Re, the correspondence of the composition is quite good [22–25]. The influence of the potential amplitude on the elemental composition of the coatings can be examined from Table 2. It can be seen that for the CrAlN and TiAlYN coatings, the ratio of metal components changes insignificantly with increasing amplitude, demonstrating a tendency to decrease the Al content.

Table 2

Effect of amplitude on multicomponent coatings composition

N	Potential parameters		Coating composition
	U, V	$U{\cdot}f{\cdot}t_p$, V	
Cathode composition – $Ti_{0.85}Si_{0.15}$			
1	0	0	$Ti_{0.92}Si_{0.08}N$
2	0.5	36	$Ti_{0.94}Si_{0.06}N$
3	1	72	$Ti_{0.96}Si_{0.04}N$
4	1.5	108	$Ti_{0.97}Si_{0.03}N$
5	2.5	180	$Ti_{0.97}Si_{0.03}N$
Cathode composition – $Ti_{0.6}Cr_{0.4}$			
6	0.5	36	$Ti_{0.45}Cr_{0.55}N$
7	1.0	72	$Ti_{0.45}Cr_{0.55}N$
8	1.5	108	$Ti_{0.45}Cr_{0.55}N$
Cathode composition – $Cr_{0.5}Al_{0.5}$			
9	0	0	$Cr_{0.48}Al_{0.52}N$
10	0.5	72	$Cr_{0.48}Al_{0.52}N$
11	1.0	144	$Cr_{0.50}Al_{0.50}N$
12	1.5	216	$Cr_{0.52}Al_{0.48}N$
13	2.0	288	$Cr_{0.51}Al_{0.49}N$
14	2.5	360	$Cr_{0.52}Al_{0.48}N$
Cathode composition – $Ti_{0.50}Al_{0.50}Y_{0.01}$			
15	0	0	$Ti_{0.46}Al_{0.54}Y_{0.01}N$
16	0.5	60	$Ti_{0.47}Al_{0.53}Y_{0.01}N$
17	1.0	120	$Ti_{0.48}Al_{0.52}Y_{0.01}N$
18	1.5	180	$Ti_{0.50}Al_{0.50}Y_{0.01}N$
19	2.5	300	$Ti_{0.52}Al_{0.48}Y_{0.01}N$

No influence of the amplitude on the elemental composition of the coatings deposited from the $Ti_{0.6}Cr_{0.4}$ cathode was found, however, the titanium content in the coatings is 1.3 times lower than in the cathode [26]. The greatest discrepancy in composition is demonstrated by coatings deposited from the $Ti_{0.85}Si_{0.15}$ cathode. In TiSiN coatings, the Si content is 2 to 5 times less than in the cathode. The higher the amplitude of the potential, the stronger the reduction [27]. Such a discrepancy in Si content is a typical problem for cathodic arc coatings based on transition metal nitrides, which complicates the possibility of their synthesis in this way.

2.2. EFFECT OF POTENTIAL PARAMETERS ON PHASE COMPOSITION, TEXTURE AND STRESS IN COATINGS

According to the data of X-ray structural analysis, the only crystalline phase that forms in coatings deposited from a titanium cathode is TiN with a cubic structure of the NaCl type. In Fig. 4,a-c show X-ray diffractograms of TiN coatings obtained under different parameters on the substrate bias potential. The ratio of peak intensities on the diffractograms differs from the data for polycrystalline TiN with chaotic crystallite orientation, according to which the (200) reflection is the most intense. Fig. 4,a shows the diffraction patterns of TiN coatings of series 1, deposited at the highest deposition rate of 20 μm/h at different bias potentials of the substrate. It can be seen that at a floating bias potential (U = 0) the most intense line is (111), that is, the orientation of crystallographic planes of the type (hhh) parallel to the surface prevails, however, this predominant orientation is not as strong as when applying a constant potential of 150 V, when a perfect axial texture is formed with the [111] axis in the direction normal to the film surface and only (111) and (222) reflections are present in the diffractogram. The calculation of texture coefficients allows you to more clearly investigate the change in texture in coatings, which are shown in Fig. 5. As the amplitude increases, the intensity ratio of the diffraction lines changes. At U>1 kV, the peak (220) remains the only reflection on the diffractograms, and its texture coefficient reaches a maximum value equal to 3 (see Fig. 5,a). Thus, the application of the pulse potential and the growth of its amplitude lead to a gradual change of the axis of the texture to [110]. The calculation of texture coefficients shows that in coatings that are deposited at a lower deposition rate (on substrates located further from the filter), a complete change of the texture axis occurs at a higher amplitude. If you vary the time parameters of the pulses at fixed amplitude of the potential at the level of 1.5 kV, the predominant orientation in the coatings does not change. In Fig. 4,b and c show the diffractograms of samples of series 2, obtained at different values of duration and frequency of pulses in the intervals 2.5…12 μs and 6…20 kHz, respectively. Line (220) is the only intense TiN line in the diffractograms of the coatings of this series.

In multicomponent coatings, one crystalline phase is also found, namely, a nitride with a cubic structure of the NaCl type. The nitride lattice parameters (a) in the coating are given in Table 1.

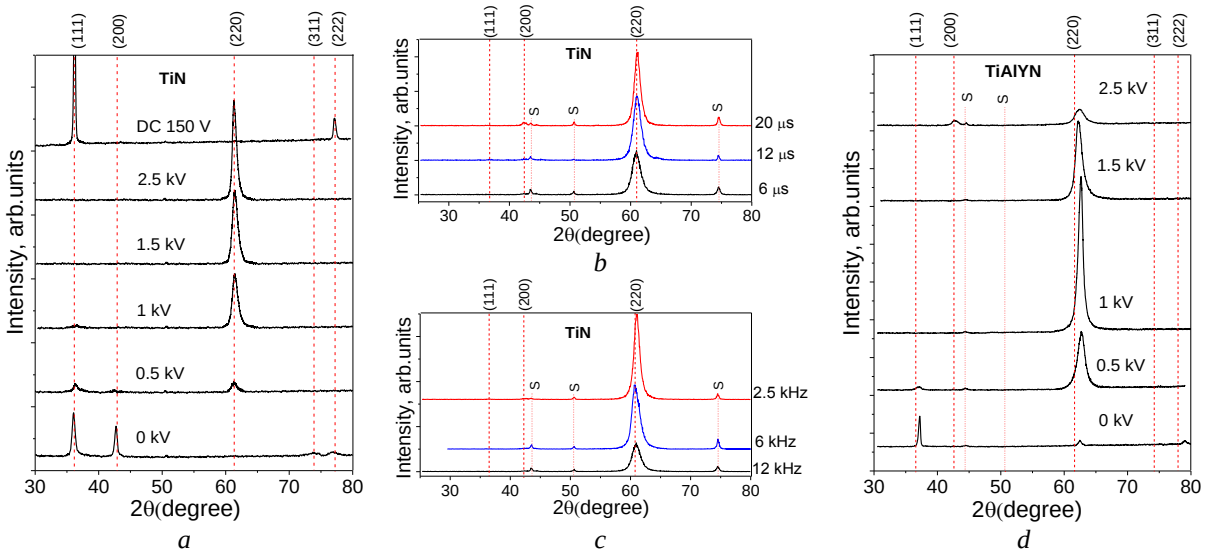

Fig. 4. X-ray diffractograms of TiN (a, b, c) and TiAlYN (d) coatings deposited at different parameters of the substrate pulse bias potential. Change in amplitude (a) at fixed values of f = 24 kHz and t_p = 5 μs. Change in pulse duration (b) at fixed values of U = 1.5 kV and f = 12 kHz. Change in the pulse frequency (c) at fixed values of U = 1.5 kV and t_p = 6 μs. Change in amplitude (d) at fixed values of f = 24 kHz and t_p = 5 μs. Dashed lines on the diffractograms show the positions of the TiN diffraction peaks. The letter "s" indicates the peaks of the substrate

Depending on the composition of the coatings, the values of the nitride crystal lattice parameters in the direction normal to the surface change almost in accordance with Vegard's rule, which indicates the formation of solid substitution solutions. All coatings deposited under a pulsed potential have a strong axial texture, the axis of which is shown in Table 1. For most coatings, the (220) reflection dominates the diffractograms, which is due to the texture formation [110]. However, in multicomponent TiZrAlNbYN coatings, another orientation prevails – [100]. In the TiAlYN and CrAlN coatings, the appearance of the [100] orientation contributes to an increase in the amplitude of the substrate pulse potential. In Fig. 4,d shows the diffractograms of TiAlYN coatings deposited at different amplitude values. Similar to TiN coatings, at a floating bias potential in TiAlYN coatings, the orientation of crystallites with (111) planes parallel to the film surface prevails. Applying a pulsed potential leads to a change in orientation to (220) – the texture axis [110]. When the amplitude of the potential increases above 1.5 kV, the orientation (220) begins to compete with (200) – the texture axis [100] (see Fig. 5,c). Similar textural changes are observed for CrAlN coatings with increasing potential amplitude (see Fig. 5,b) [22–25, 28].

Important structural characteristics that significantly affect the hardness and mechanical properties of protective coatings are the size of crystallites and the level of residual stresses, the results of which are determined in Table 1 and Fig. 6. The size of the crystallites in the coatings is in the range of 5…32 nm and varies depending on the parameters of the potential, the composition of the coating and the rate of its deposition. For most systems, the application of a pulsed potential leads to a sharp decrease in crystallite size up to 2 times compared to a floating potential. With further growth of the potential amplitude or pulse filling factor, the changes are not so significant. X-ray tensometry revealed residual compressive stresses varying from 3 to 11 GPa in all coatings. For TiN coatings, it was found that when the amplitude of the pulse potential increases, the level of compressive stresses changes non-monotonically: first it increases, and then (at U > 0.5 kV) it decreases. Similar non-monotonic voltage changes are observed if the amplitude is fixed at 1.5 kV and the time characteristics of the pulses are changed. A decrease in stress is observed when the duty cycle exceeds 10%. The analysis of the obtained results showed that the key factor that affects the size of crystallites and the level of compressive stresses in coatings is the average value of the bias potential during deposition, which can be characterized by the parameter ($U{\cdot}f{\cdot}t_p$). For TiN coatings, the maximum stresses of 9…11 GPa are reached at ($U{\cdot}f{\cdot}t_p$) near 60 V, and with a further increase in the parameter, stress relaxation occurs. The degree of stress reduction and the size of the crystallites largely depend on the rate of coating deposition. A higher deposition rate ensures a lower stress level (see Fig. 6,d) and a larger size of crystallites in the coating (see Fig. 6,a). For CrTiN and CrAlN coatings, the maximum on the stress curve is wider and shifted towards higher values ($U{\cdot}f{\cdot}t_p$) compared to TiN (Fig. 6,e), while it is not found for TiAlYN (Fig. 6,f). For multicomponent coatings with limited solubility of CrAlN and TiAlYN components, the course of the compressive stress change curves with increasing parameter ($U{\cdot}f{\cdot}t_p$) has a significant feature. At high values of the parameter, the residual compressive stresses do not decrease, but increase (see Fig. 6,e,f). Such differences are caused by a number of factors. The most significant is the possibility of disintegration of the supersaturated solid solution, which causes an increase in the specific volume of the coating fixed on the substrate.

Thus, the change in pulse potential parameters has a significant impact on the microstructure, texture and stress state of nitride coatings, which is agreement with

data from other studies [29–33]. It is known that during coating deposition, the supply of high voltage pulses with duration of 20 μs can lead to a significant decrease in compressive stress. Stress reduction can be achieved by increasing both the bias potential amplitude from 1.7 to 20 kV and the pulses frequency from 0.22 to 1.2 kHz. The stresses in TiN coating decrease exponentially from 8 to 2 GPa with the increase in the parameter $(U{\cdot}f)$ [10, 29].

The effect of the amplitude of the pulsed bias potential with frequency of 10 kHz was studied during deposition of TiN and $Ti_{1-x}Al_xN$ coatings [16, 32]. To maintain the level of energy release due to ion bombardment, on the same level, with increasing amplitude, the pulse duration varied in the range of 2…40 μs so that the value of the parameter $U{\cdot}f{\cdot}t_p$ was kept constant 200 V. It was found that as the amplitude of the pulse bias increased from 0 to 4 kV, the stress changed nonmonotonically in TiN coatings, reaching the maximum value at the amplitude of 0.5 kV. The change in the stress level associated with the increase in the ion energy under the action of the high voltage bias potential is accompanied by a change in the preferred orientation of the nitride grains in the coatings from (111) to (220), and then to (200). In another study, transitions between the (111), (220), and (200) texture in TiN coatings are determined not only by the value of the bias potential amplitude, but also by its frequency [33].

However, the effect of deposition rate on the characteristics of nitride coatings deposited by pulsed substrate bias has not been studied earlier. Presently, the influence of the deposition rate on the stress level, the degree of their relaxation, and the size of coherent diffracting domains is clearly seen. This effect can be explained by the fact that in addition to the energy of the particles forming the film, the important parameter that determines the mechanism of their growth is the temperature of the deposition surface. In these experiments, the change in the ion flux affects the temperature. If we compare the results of different authors, it is impossible to construct simple correlations between the parameters $f{\cdot}t_p$ or $U{\cdot}f{\cdot}t_p$ and the magnitude of the stresses, since the temperature of the deposition surface also significantly affects their level. The increase in deposition rate leads to increased radiation-stimulated surface heating.

Structure of coatings deposited by ion-plasma methods is determined, on the one hand, by the ion flow parameters (ion energy and ion flow density), and on the other, by the temperature of the substrate, pressure, and the state of the reactive gas that interacts with the ions [1, 18, 34, 35].

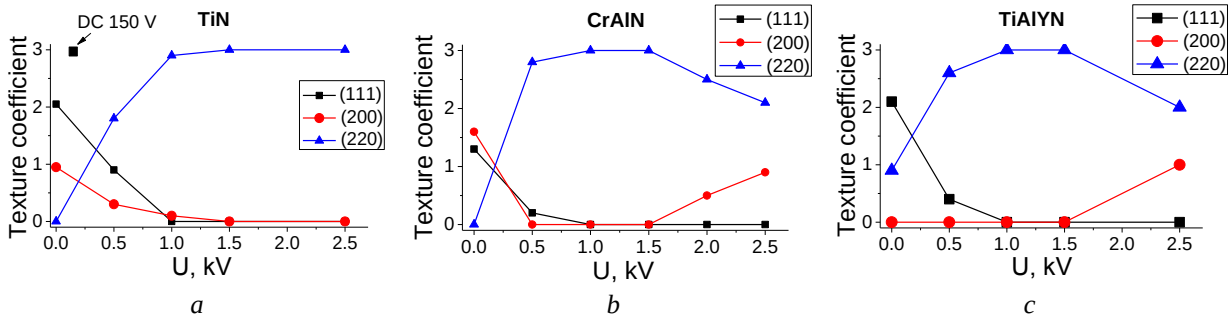

Fig. 5. Texture coefficients of nitride with an fcc structure of the NaCl type for coatings of different elemental composition depending on the amplitude of the pulse potential U

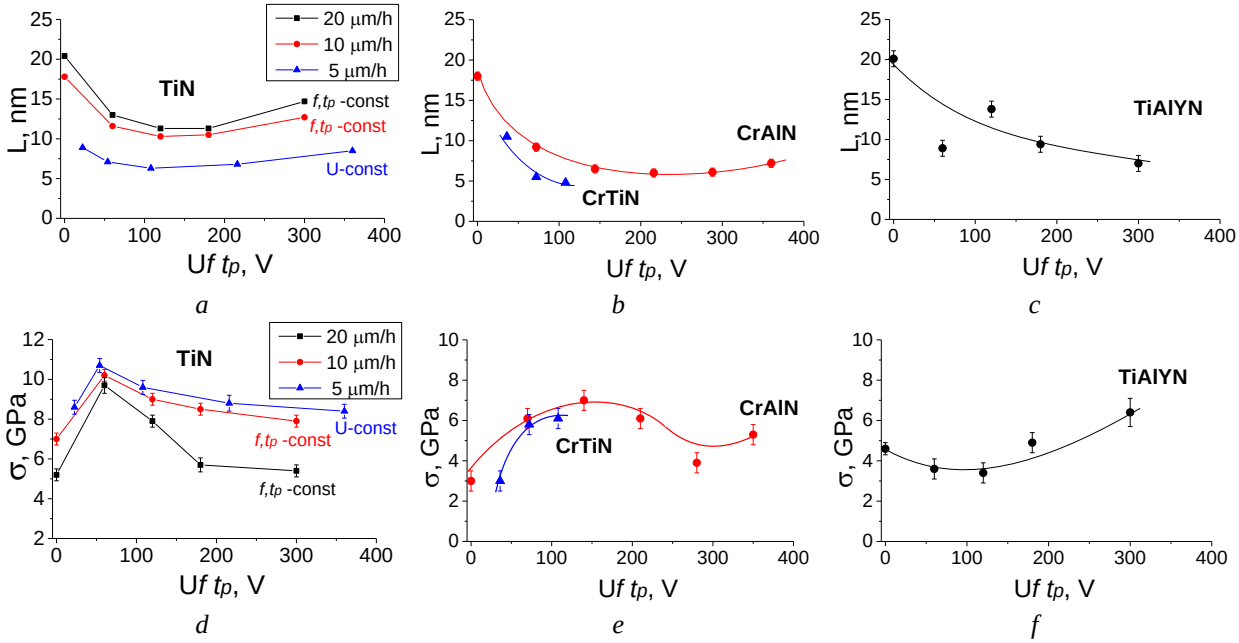

Fig. 6. Nitride crystallite size (a–c) and compressive stress (d–f) in coatings of different elemental composition depending on the $U{\cdot}f{\cdot}t_p$ (a–f) and deposition rate (a, d)

In the process of formation, the so-called high-energy condensation mode is implemented, when the particles forming the film have hyperthermal energy that exceeds the displacement energy of atoms E_d. This makes it possible for ions to penetrate into the subsurface region, which is associated with the compaction of coatings, the formation of compressive stresses and metastable phases in them [8–10]. The main part of the coating deposition process occurs between potential pulses, and at the moment of the pulse, the processes of ion implantation, sputtering, and radiation-stimulated annealing of the already formed coating layers prevail.

Previously, pulses were used to reduce the level of high stresses, which are characteristic for cathodic arc coatings and can be the cause of low operational properties and even their destruction. Stresses in cathodic arc coatings are considered as the sum of the thermal component associated with the difference in the coefficients of thermal expansion of the coating and the substrate, and the compressive stresses of growth due to densification under the influence of ion bombardment [14]. Due to the low temperature of the deposition, which takes place at the pulse potential, the growth stresses significantly prevail over the thermal ones. The reduction of growth stresses with increasing potential and, accordingly, the energy of the ions agrees well with the modified Davis model [36], according to which there is a competition between two processes: the generation of compressive stresses due to the implantation of ions and the relaxation of stresses during the migration of defects in nonlocal thermoelastic peaks (NTP) of ions [17, 20, 37]. Later, it was shown that the pulse potential affects not only the stress level, but also the coating microstructure, substructure parameters and texture. It has been reliably established that there are correlations between the stress level and the texture in the coatings, which is explained by the provision of a minimum of total free energy [34].

Deposition of nitride coatings from flows of filtered cathodic arc plasma is carried out at a relatively low nitrogen pressure (~ 0.1 Pa). Under these conditions, the interaction of plasma ions with the gas on the way from the cathode to the deposition surface does not significantly affect their charge and energy state. The energy of metal ions E bombarding the growth surface during deposition is determined by their initial energy E_0, with which the ions leave the cathode, and the energy acquired due to application the negative bias potential [1, 2]: $E = E_0 + ieU$, where i – the multiplicity of the charge of the ion; U – substrate potential; e – elementary charge. Cathodic arc plasma ions generated by the cathode are characterized by a certain charge and energy state distribution depending on the atomic number of the cathode material element. The average values of the charge and energy of the ions change in the intervals of 1…3 and 20…150 eV, respectively, showing a correlation with the value of the cohesion energy [38]. Not only the potential of the substrate, but also the composition of the cathode is important in controlling the energy of the deposited ions. In particular, with the same potential parameters, the average energy of multi-charged ions of heavy elements (Zr, Nb, Y, Re) is 2–3 times higher than that of Ti and Al ions. It is this to a large extent that determines the differences in the influence of potential parameters on the structural characteristics of coatings of different composition. At the same time, when analysing, the difference in the homologous deposition temperature of the coatings (the ratio between the deposition temperature and the nitride melting temperature) should not be neglected. Of all investigated metal nitrides, chromium nitride has the lowest melting point, and aluminum ions have the lowest average energy. It was when cathodes containing Cr and Al were used that the coatings had a lower stress level and changed the predominant orientation with increasing amplitude.

Special attention should be paid to the impact of the deposition rate (ion flux density) on the stress level, the degree of their relaxation, and the size of the crystallites. This effect can be explained by the fact that, in addition to the energy of the ions forming the coating, the temperature of the deposition surface is an important parameter that determines the mechanism of their growth. In these experiments, the change in the deposition rate affects the temperature. An increase in deposition rate leads to an increase in radiation-stimulated heating of the surface. The difference in surface temperature in the experiments does not exceed 200 °C, however, in the conditions of high-energy ion bombardment, this is enough to ensure the conditions necessary for reducing the stress level, increasing the crystal size, and changing the texture in the coatings. These findings are consistent with theoretical calculations within the thermoelastic thermal peak model. With increasing energy, relaxation processes in the coatings associated with annealing of excess interstitial atoms, stress reduction, and texture change are activated when the peak temperature exceeds 1/3 of the melting point T_m [34]. The intensity of the relaxation processes largely depends on the radiation heating of the deposition surface and increases significantly at temperatures above 100 °C, which is ensured at a fairly high ion flux density (> 10^{16} ions/(cm^2·s) at U ~ 1 kV). The optimal range of the pulse duty sycle, which allows for stress relaxation without significantly reducing the deposition rate and excessive heating of the surface, is 10…20%. The disadvantage of calculations within the model of thermal peaks is the fact that they do not take into account the possibility of phase transformations in coatings.

2.3. CONTROL OF THE MECHANICAL PROPERTIES OF COATINGS

High-quality wear-resistant coatings require a combination of strength, hardness and the ability to recover. Hardness and elasticity are of equal importance for increasing wear resistance, especially in complex processes associated with shock loading and erosion. An important feature of hard nanocrystalline coatings is that materials with high hardness H can significantly differ in the values of elasticity modulus E. The combination of high hardness and low modulus of elasticity is considered optimal. Numerical values of these characteristics are usually determined by the method of nanoindentation. The H/E ratio is often used to

characterize a material's resistance to elastic fracture deformation [5]. The results of coatings nanoindentation are shown in Table 1 and Fig. 7. All investigated coatings are characterized by sufficiently high hardness H in the range of 25…36 GPa and Young's modulus E in the range of 350…450 GPa. The *H/E* ratio is 0.7…0.9, which is typical for nanostructures and significantly exceeds the values characteristic of coarse-crystalline materials $H/E < 0.04$. The hardness of multicomponent coatings does not differ significantly from the hardness of TiN coatings, as does the *H/E* value. Changing the parameters of the bias potential or the deposition rate has little effect on the hardness of the coatings. The greatest effect was found for the coatings of the TiAlYN system. When the parameter ($U \cdot f \cdot t_p$) increases from 0 to 300 V, the hardness of TiAlYN coatings decreases from 36 to 25 GPa, which is due to the decomposition of the saturated solid solution with the formation of amorphous phases during intense ion bombardment of the surface.

The results of cavitation and abrasion tests of coatings of different compositions deposited at pulsed bias potential showed that the addition of components reduces the average rate of both types of wear [23, 24, 39, 40]. The abrasive wear rate of alloyed coatings is three orders of magnitude lower than that of uncoated steel and an order of magnitude lower than the wear rate of TiN. The abrasion resistance of the TiAlYN coating is 30% lower than that of the best coatings of other systems. Cavitation resistance of TiN coatings is also the worst. After tests, a small number of large ulcers are observed on their surfaces, which reach the substrate in 1.5 h due to the sufficiently pronounced columnar structure of the coating. Doping coatings based on TiAlN with a small amount of Y and Re is the most effective, which significantly slows down both the rate of surface erosion and the rate of erosion spreading deep into the coating. The average rate of cavitations wear of such coatings is 10–12 times lower than that of TiN, and the penetration time of cavitation defects to the substrate increases to 12…14 h. In addition, when annealed in vacuum, most multicomponent coatings retain high hardness, in contrast to TiN coatings, the hardness of which decreases to 25 GPa.

A change in potential parameters during deposition has a significant impact on the adhesion and wear resistance of coatings. In Fig. 8 shows the results of adhesion and tribological tests of TiN coatings deposited at different bias potentials on the substrate [21]. Scratch tests were performed to determine the adhesion strength of the coatings. The moment of destruction of the coatings was determined by the change in the intensity of the acoustic emission and the force friction force, as well as visually using the analysis of electron microscopic images of scratches after the tests. Fig. 8,a,b illustrate the surface of the samples after the tests. For a coating with a strong texture (111), synthesized at a constant bias potential, the formation of cracks and exfoliation is observed, which is characteristic for hard brittle coatings deposited on hardened substrates (see Fig. 8,a). Coatings with a texture (220), synthesized at a pulse bias potential on the substrate, demonstrate a fundamentally different behavior. Cracking begins in the form of lateral cracks along the edges of the scratch (see Fig. 8,b), and the values of critical loads corresponding to the beginning of coating destruction are 1.5–2 times higher than at constant potential. The coating deposited at a potential of 0.5 kV demonstrated the best adhesion. The acoustic emission levels of this coating are extremely low, despite the clear pattern of cracks within the scratch mark observed. This is a sign of the formation of cracks that are located within the coating and do not reach the intermediate layer of the coating - substrate. Imperfect texture and high stress levels contribute to this behavior. With the growth of the potential amplitude, which is accompanied by the improvement of the texture, the reduction of stresses and more pronounced columnarity, the adhesion of the coatings deteriorates somewhat, since the formed cracks are able to spread faster through the boundaries of the columns. However, in the amplitude range of 1…1.5 kV, the adhesion will remain sufficiently high.

Dependencies of the friction coefficient of TiN coatings deposited at different substrate bias potentials on the distance traveled during tribological tests are shown in Fig. 8,c. It can be seen that the coatings deposited at a pulsed potential have significantly better tribological properties than the coating obtained at a constant one. During the tests, the coefficient of friction of the coating obtained at a potential of 150 V rapidly increases from 0.05 to 0.8. The coefficient of friction of coatings deposited at pulsed potential does not change significantly during the tests and remains at a rather low level of 0.1–0.2. The width and depth of wear tracks during tribological tests of these coatings are 3–4 times smaller. A significant improvement in properties is primarily due to changes in the predominant grain orientation and microstructure. The high coefficient of friction of the coating deposited at a constant potential can be caused by a large number of wear products formed due to light chipping along the densely packed planes (111) and serving as an abrasive.

For multi-component coatings, the positive effect from the application of a pulse bias potential was no less significant. Fig. 9 shows the results of cavitation and abrasion tests of TiAlYN coatings obtained at a constant bias potential of 150 V and different amplitude of the pulse potential. Supplying a pulsed potential and increasing its amplitude contribute to a 3–5 times decrease in the rate of coatings cavitation wear (see Fig. 9,a) compared to a constant potential. At the same time, the number and depth of erosion defects on the surface is sharply reduced. Similar to the TiN coating, such changes are largely due to changes in texture. With potential amplitude in the range of 0.5…1.5 kV, a small number of ulcers are observed on the eroded surface (see Fig. 9,d). At an amplitude of 2.5 kV, the general picture of the eroded surface resembles the surface of the coating obtained at a constant potential (see Fig 9,d), but with a much lower density of defects in the form of ulcers and cracks (see Fig. 9,e). Despite the similarity of the general pattern of destruction, the time of formation of through defects in the coating deposited at amplitude of 2.5 kV is twice as long as at a constant potential.

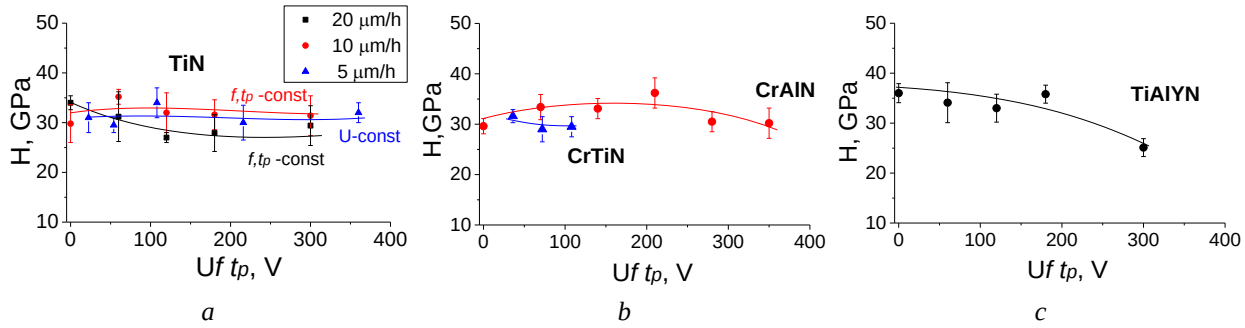

a *b* *c*

Fig. 7. Hardness of coatings of different elemental composition depending on the parameter $U \cdot f \cdot t_p$ (a–c) and deposition rate (a)

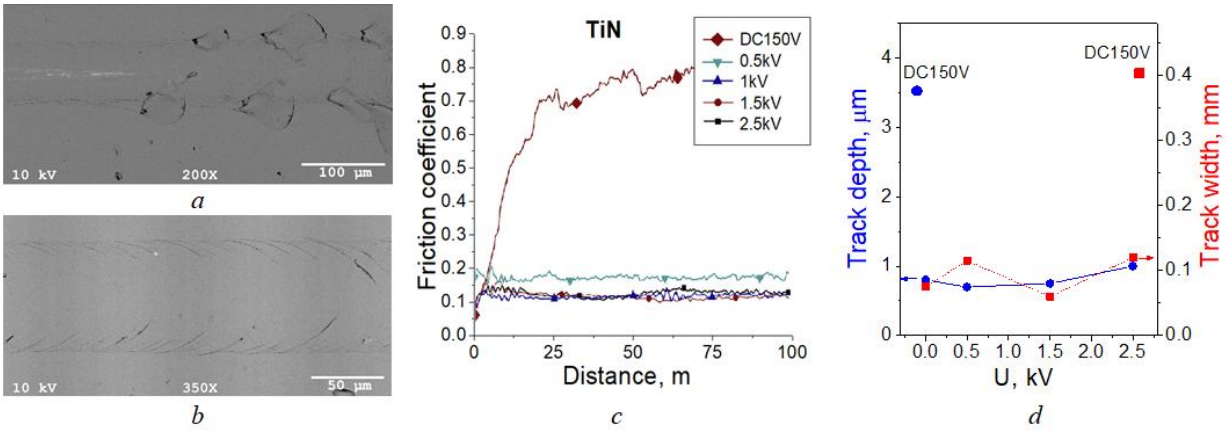

a *b* *c* *d*

Fig. 8. Results of adhesion and tribological tests of TiN coatings. Electron microscopic images of a scratch test mark of coatings deposited at constant 150 V (a) and pulsed 0.5 kV (b) bias potentials. Effect of the potential on the coefficient of friction (c), width and depth of wear tracks after tribological tests of coatings (d)

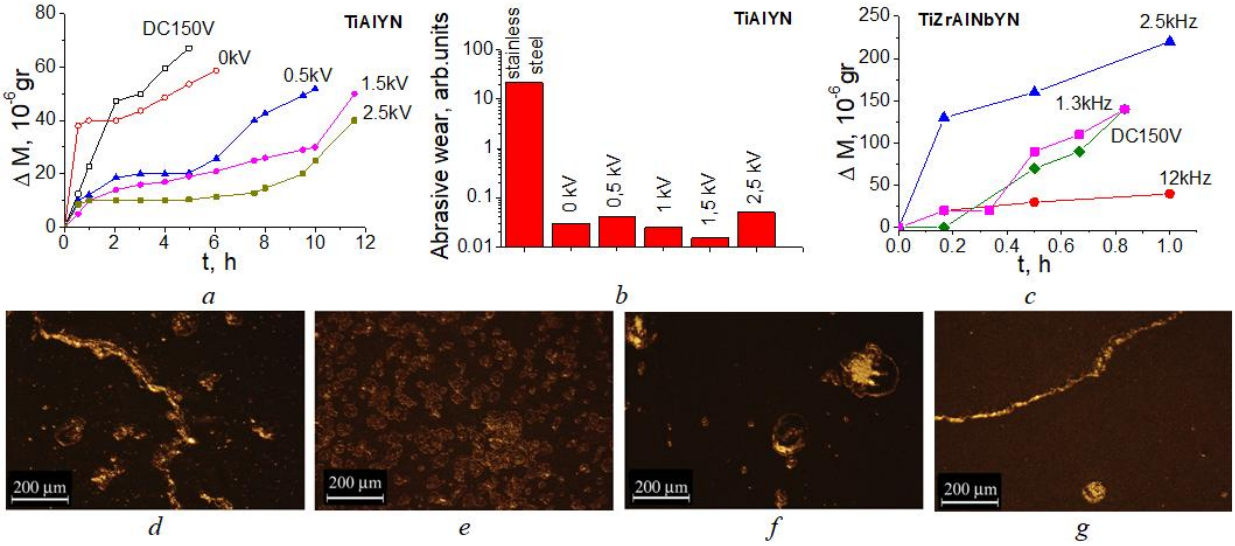

a *b* *c* *d* *e* *f* *g*

Fig. 9. Results of cavitation and abrasion tests of multicomponent nitride coatings, obtained at a constant bias potential of 150 V and different parameters of the pulse potential on the substrate. Effect of change of potential amplitude on kinetic curves of cavitation wear (a) and abrasive wear rate (b) of TiAlYN coatings. The effect of changing the pulse frequency on the kinetic curves of cavitation wear (c) of TiZrAlNbYN coatings. Microscopic images of cavitation damage on the surface of TiAlYN coatings deposited at a constant bias potential of 150 V (d) and pulse potential amplitude of 0 kV (e), 0.5 kV (f), and 2.5 kV (g)

Although the hardness of this coating is only 25 GPa. The results of tests of TiAlYN coatings for abrasion resistance are presented in Fig. 9,b. The best resistance was demonstrated by coatings deposited at a potential of 1.5 kV. For the coating deposited at a potential of 2.5 kV, which showed the best cavitation resistance, the abrasive wear was almost 3 times higher, which is due to the reduced hardness and higher surface roughness. The obtained results do not make it possible to reveal an unambiguous correlation between the resistance of coatings to different types of wear, their hardness and the *H/E* parameter. If the problem of the interaction of two bodies with rough surfaces is considered, it is the *H/E* parameter together with the

roughness of the contacting surfaces that determines the mode of interaction of these bodies (plastic or elastic deformation takes place in the contact zone). Here, high hardness does not guarantee a significant service life of the coating. Other processes take place during the cavitation effect, when erosion occurs under the action of shock waves with high pressure and high speed of microjets, which arise in the process of collapsing cavitation gas bubbles. In experiments on the impact of cavitation, the most destructive factor is wear caused by impacts of eroded solid particles of the coating material. Therefore, the wear resistance of the coating is determined by its level of adhesion to the substrate. It can decrease with poor adhesion, a high level of residual stresses and the presence of macrodefects and foreign inclusions, which, as a rule, are the initial points of destruction.

In this work, coatings deposited from filtered plasma, that is, with a minimum number of macrodefects, were studied. Under these conditions, the role of residual stresses in the prediction of wear resistance is dramatically increased. Compressive stresses were detected in all obtained coatings. The maximum stress level of 7.5 GPa is observed in the coating deposited at a constant potential of 150 V. Obviously, high wear and cracking of this sample due to cavitation is associated with increased stresses. In all coatings synthesized at pulsed potential, the stress level is lower. The dependence of stress on the amplitude of the pulse potential is non-monotonic with a minimum at 1 kV. When the amplitude increases to 2.5 kV, the stress level again becomes quite high and, despite the low cavitation wear, cracks are visible on the surface of the sample after the tests. In coatings obtained at an amplitude in the range of 0.5…1.5 kV, which demonstrate high resistance, both during cavitation and during abrasive tests, stresses do not exceed 5 GPa. The obtained results show that when predicting the wear resistance of coatings, one cannot limit oneself to one of the criteria, but must take into account a complex of interrelated factors: hardness, *H/E* parameter, residual stress level, crystallite size, texture, surface roughness, degree of columnar microstructure.

Similar conclusions are confirmed by the results of cavitation tests of TiZrAlNbYN coatings with texture (200). Indeed, although an increase in the frequency of bias potential pulses on the substrate does not significantly affect the hardness of the coatings, it has a clear effect on the cavitation stability of the samples (see Fig. 9,c). The highest cavitation wear, which means the worst resistance, was demonstrated by the non-uniform and stressed coating obtained at a frequency of 2.5 kHz, which had the most non-uniform structure with well-defined through fibers. The coating obtained at a frequency of 1.3 kHz turned out to be more stable. Its stability is close to that of a coating deposited at a constant bias potential. The coating with the most homogeneous and finely dispersed nanostructure, which was deposited at a frequency of 12 kHz, had the best resistance. The microscopic image of the fracture of this coating is similar to the dense needle-like structure of TiAlYN coatings, which demonstrated high wear resistance (see Fig. 2,c).

CONCLUSIONS

The structure and properties of protective cathodic vacuum arc coatings based on TiN and CrN, including multi-component ones with the addition of Al, Si, Zr, Y, Re, Nb, Hf, deposited using a rectilinear magnetoelectric filter at different substrate bias potentials, were studied. The applied design of the filter demonstrates good quality of metal plasma filtration from microparticles at a high coatings deposition rate. With different modes of application of the substrate bias potential the deposition of nitride-based coatings with a nanocrystalline cubic structure (of the NaCl type), close to stoichiometric nitrogen content and high hardness of 25…36 GPa is obtained.

Changing the characteristics of the high voltage pulse bias potential in the range: amplitude 0.5…2.5 kV, duration 5...20 μs, repetition frequency 1.3…24 kHz, allows you to effectively control the morphology, crystallite size, texture, stress level in coatings, which effects on their mechanical properties. It was found that the potential parameters have little effect on the elemental composition of coatings deposited using cathodes of Ti, $Ti_{0.5}Al_{0.5}$ (including with the additions of up to 2 at.% Y and Re), $Ti_{0,48}Zr_{0,18}Al_{0,18}Nb_{0,09}Y_{0,07}$, $Ti_{0.6}Cr_{0.4}$, and $Cr_{0.5}Al_{0.5}$. The Al concentration in the coatings corresponds well to the cathode, in contrast to Si concentration, which greatly decreases with increasing potential.

As the potential amplitude increases, the texture axis in the coatings changes in the sequence [111]→[110]→[100]. The level of compressive stresses, the size of the crystallites and the surface roughness of the coatings depend on the parameter ($U \cdot f \cdot t_p$), which characterizes the average value of the bias potential, which means the average energy of the plasma ions during deposition. The intensity of the relaxation processes in coatings associated with the annealing of excess interstitial atoms, stress reduction, and texture change largely depends on the radiation heating of the deposition surface due to ion bombardment, and increases significantly with an increase in the deposition rate. Differences in the influence of parameters on the level of residual stresses for coatings of different compositions are due to the difference in the average energy of cathodic plasma ions and the formation of metastable solid solutions and amorphous phases in coatings with limited solubility.

The application of bias pulse potential with an amplitude of 1…2 kV, frequency of 10…20 kHz and duty cycle of 10…15% makes it possible to form a homogeneous dense nanostructure with a predominant [110] or [100] orientation and a low stress level 4…5 GPa and defects in coatings of different compositions. It is shown that such structure provides improved the coatings resistance to various types of wear. Unequivocal correlations were not found between the hardness of the coatings, the modulus of elasticity and their wear.

REFERENCES

1. I.I. Aksenov, A.A. Andreev, V.A. Belous, V.E. Strel'nitskij, V.M. Khoroshikh. *Vacuum arc: plasma sources, coating deposition, surface modification.* Kiev: “Naukova dumka”, 2011, 724 p.

2. A. Anders. *Cathodic Arcs: From Fractal Spots to Energetic Condensation*. New York: “Springer Inc.”, 2008, 544 p.

3. P.M. Martin. *Introduction to Surface Engineering and Functionally Engineered Materials*. New York: “Wiley-Scrivener”, 2011, 568 p.

4. S. Veprek, P. Holubar, M. Veprek-Heijman. Industrial Applications of Hard and Superhard Nanocomposite Coatings on Tools for Machining, Forming, Stamping and Injection Molding // *Advanced Materials Research*. 2016, v. 1135, p. 218-233.

5. A. Gavaleiro, J.T. De Hosson (Eds). *Nanostructured Coatings*. New York: “Springer”, 2006, 648 p.

6. E.N. Reshetnyak, V.E. Strel’nitskij. Synthesis of hardening nanostructural coatings // *Problems of Atomic Science and Technology*. 2008, N 2, p. 119-130.

7. A. Anders. A structure zone diagram including plasma-based deposition and ion etching // *Thin Solid Films*. 2010, v. 518, p. 4087-4090.

8. D. Manova, J.W. Gerlach, S. Mandl. Thin Film Deposition Using Energetic Ions // *Materials*. 2010, v. 3, p. 4109-4141.

9. A. Anders. *Handbook of plasma immersion ion implantation and deposition*. New York: “Wiley”, 2000, 736 p.

10. M. Bilek, D. Mc Kenzie, W. Moeller. Use of low energy and high frequency PBII during thin film deposition to achieve relief of intrinsic stress and microstructural changes // *Surface and Coatings Technology*. 2004, v. 186(1-2), p. 21-28.

11. J. Pelletier, A. Anders. Plasma-based ion implantation and deposition: A review of physics, technology, and applications // *IEEE Transactions on Plasma Science*. 2005, v. 33, p. 1944-1959.

12. D.S. Aksyonov, I.I. Aksenov, V.E. Strel’nitskij. Filtered vacuum arc erosive plasma sources: a review // *Problems of Atomic Science and Technology*. 2007, N 2(90), p. 191-203.

13. V.V. Vasylyev, A.A. Luchaninov, V.E. Strel’-nitskij. High-productive source of the cathodic vacuum-arc plasma with the rectilinear filter // *Problems of Atomic Science and Technology*. 2014, N 1(89), p. 97-100.

14. G. Abadias. Stress and preferred orientation in nitride-based PVD coatings // *Surface and Coatings Technology*. 2008, v. 202, №11, p. 2223-2235.

15. S. Mahieu, D. Depla. Reactive sputter deposition of TiN layers: modelling the growth by characterization of particle fluxes towards the substrate // *Journal of Physics D: Applied Physics.* 2009, v. 42, N 5, p. 053002.

16. S. Mukherjee, F. Prokert, E. Richter, W. Moeller. Comparison of TiN and $Ti_{1-x}Al_xN$ coatings deposited on Al using plasma mmersion ion implantation assisted deposition // *Surface and Coatings Technology*. 2005, v. 200, N 7, p. 2459-2464.

17. V.V. Vasyliev, A.I. Kalinichenko, E.N. Reshetnyak, G. Taghavi, Pourian Azar, M. Ürgen, V.E. Strel'nitskij. Experimental and modeling study on the role of Ar addition to the working gas on the development of intrinsic stress in TiN coatings produced by filtered vacuum-arc plasma // *Thin Solid Films*. 2017, v. 642, p. 207-213.

18. V.V. Vasil’ev, A.A. Luchaninov, E.N. Reshetnyak, V.E. Strel’nitskij, G.N. Tolmatcheva, M.V. Reshetnyak. Structure and hardness of Ti-N and Ti-Si-N coatings deposited from the filtered vacuum-arc plasma // *Problems of Atomic Science and Technology*. 2009, N 2(93), p. 173-180.

19. I.I. Aksenov, D.S. Aksyonov, A.A. Andreev, V.A. Belous, O.V. Sobol. *Vacuum arc coatings. Technology, materials, structure, properties*. Kharkiv: NSC KIPT, 2015, 349 p.

20. A.I. Kalinichenko, E.N. Reshetnyak V.E. Strel’-nitskij. Influence of bias potential and substrate orientation on characteristics of deposited coating: the role of sputtering // *East European Journal of Physics*. 2018, v. 5, N 2, p. 54-61.

21. S.S. Akkaya, V.V. Vasyliev, E.N. Reshetnyak, K. Kazmanlı, N. Solak, V.E. Strel'nitskij, M. Ürgen. Structure and properties of TiN coatings produced with PIII&D technique using high efficiency rectilinear filter cathodic arc plasma // *Surface and Coatings Technology*. 2013, v. 236, p. 332-340.

22. V.A. Belous, V.V. Vasyliev, V.S. Goltvya-nytsya, S.K. Goltvyanytsya, A.A. Luchaninov, E.N. Reshetnyak, V.E. Strel’nitskij, G.N. Tolmacheva, O. Danylina. Structure and properties of Ti-Al-Y-N coatings deposited from filtered vacuum-arc plasma // *Surface and Coatings Technology.* 2011, v. 206, N 7, p. 1720-1726.

23. V.V. Vasyliev, V.S. Goltvyanytsya, S.K. Goltvyanytsya, A.A. Luchaninov, V.G. Marinin, E.N. Reshetnyak, V.E. Strel'nitskij, G.N. Tolmachova. Durability of the multicomponent nitride coatings based on TiN and (Ti,Al)N deposited by PIII&D method // *Problems of Atomic Science and Technology*. 2015, N 2 (96), p. 130-138.

24. V.V. Vasyliev, A.A. Luchaninov, E.N. Reshetnyak, V. E.Strel’nitskij, G.N. Tolmacheva, G.A. Pribytkov, V.V. Korzhova. Structure and properties of nitride coatings deposited from filtered vacuum-arc plasma using $Cr_{0.5}Al_{0.5}$ powder cathode // *Journal of Surface Physics and Engineering*. 2016, v. 1, N 1, p. 62-80.

25. V. Vasyliev, A. Luchaninov, E. Reshetnyak, V. Strel’nitskij, B. Lorentz, S. Reichert, V. Zavaleyev, J. Walkowicz, M. Sawczak. Structure and properties of the (Cr, Al)N coatings deposited by PIII&D method // *Problems of Atomic Science and Technology*. 2016, N 6(106), p. 244-247.

26. V. Vasyliev, A. Kalinichenko, F. Komarov, S. Konstantinov, A. Luchaninov, E. Reshetnyak, V.E. Strel’nitskij. Structure and properties of nitride coatings based on Ti and Cr synthesized by PIII&D technique / Pogrebnjak A., Bondar O. (eds.). *Microstructure and Properties of Micro- and Nanoscale Materials, Films, and Coatings (NAP 2019)*. Singapore: “Springer”, 2020, p. 91-104.

27. V.V. Vasyliev, A.A. Luchaninov, E.N. Reshetnyak, V.E. Strel’nitskij, G.N. Tolmacheva, G.A. Pribytkov, A.V. Gurskikh, M.G. Krinitcyn. Application of powder cathodes for Ti-Si-N coatings deposition from

the filtered vacuum-arc plasma // *Physical Surface Engineering*. 2015, v. 13, N 2, p. 149-163.

28. E. Reshetnyak. Structure and stress state of TiN and $Ti_{0.5-x}Al_{0.5}Y_xN$ coatings prepared by the PIII&D technique from filtered vacuum-arc plasma // *Problems of Atomic Science and Technology*. 2014, N 1, p. 159-162.

29. M. Bilek, D. McKenzie, R. Tarant, S. Lim, D. McCulloch. Plasma-based ion implantation utilising a cathodic arc plasma // *Surface and Coatings Technology*. 2002, v. 156, N 1-3, p. 136-142.

30. S. Heinrich, S. Schirmer, D. Hirsch, J.W. Gerlach, D. Manova, W. Assmann, S. Mändl. Comparison of ZrN and TiN formed by plasma based ion implantation & deposition // *Surface and Coatings Technology*. 2008, v. 202, N 11, p. 2310-2313.

31. S. Lim, D. McCulloch, M. Bilek, D. McKenzie. Relation between microstructure and stress in titanium nitride films grown by plasma immersion ion implantation // *Journal of Applied Physics.* 2003, v. 93, N 7, p. 4283-4288.

32. S. Mukherjee, F. Prokert, E. Richter, W. Moeller. Compressive stress, preferred orientation and film composition in Ti-based coatings developed by plasma immersion ion implantation-assisted deposition // *Surface and Coatings Technology*. 2004, v. 186, N 1-2, p. 99-103.

33. S. Mandl, G. Thorwarth, B. Stritzker, B. Rauschenbach. Two-dimensional texture and sheath evolution in metal plasma immersion ion implantation // *Surface and Coatings Technology*. 2005, v. 200, N 1-4, p. 589-193.

34. A. Kalinichenko, E. Reshetnyak, V. Strel'nitskij, G.Abadias. Role of nonlocal thermoelastic peaks in the stress and texture evolution of TiN coatings formed by plasma based ion implantation and deposition // *Surface and Coatings Technology*. 2020, v. 391, p. 125695.

35. V.V. Vasil'ev, A.A. Luchaninov, E.N. Reshetnyak, V.E. Strelnitskij. Effect of substrate position relative to the flow of filtered cathodic-arc plasma on the structure and properties of TiN coatings // *Problems of Atomic Science and Technology*. 2017, N 2(108), p. 160-167.

36. C.A. Davis. A simple model for the formation of compressive stress in thin films by ion bombardment // *Thin Solid Films*. 1993, v. 226, N 1, p. 30-34.

37. A.I. Kalinichenko, S.S. Perepelkin, E.N. Reshetnyak, V.E. Strel'nitskij. Effect of time parameters of pulsed bias potential on intrinsic stress in TiN coating deposited from inclined ion beam // *Problems of Atomic Science and Technology*. 2018, N 1(113), p. 114-117.

38. A. Anders. The evolution of ion charge states in cathodic vacuum arc plasmas: a review // *Plasma Sources Science and Technology* 2012, v. 21, p. 035014.

39. V. Belous, V. Vasyliev, A. Luchaninov, V. Marinin, E. Reshetnyak, V. Strel'nitskij, S. Goltvyanytsya, V. Goltvyanytsya. Cavitation and abrasion resistance of Ti-Al-Y-N coatings prepared by the PIII&D technique from filtered vacuum-arc plasma // *Surface and Coatings Technology*. 2013, v. 223, p. 68-74.

40. V.V. Vasyliev, V.I. Kovalenko, A.A. Luchaninov, V.G. Marinin, E.N. Reshetnyak, V.E. Strel'nitskij, G.N. Tolmachyova. Mechanical properties and erosion resistance of the vacuum-arc coatings (Ti, Al)N modified with yttrium // *Problems of Atomic Science and Technology*. 2011, N 4, p. 160-164.

Article received 02.12.2023

ВПЛИВ ІМПУЛЬСНОГО ПОТЕНЦІАЛУ ЗМІЩЕННЯ ПІДКЛАДКИ НА СТРУКТУРУ ТА ВЛАСТИВОСТІ НІТРИДНИХ ПОКРИТТІВ, ОСАДЖЕНИХ З ФІЛЬТРОВАНОЇ КАТОДНО-ДУГОВОЇ ПЛАЗМИ

О.М. Решетняк, В.Є. Стрельницький, В.В. Васильєв, О.А. Лучанінов

Наводяться результати досліджень покриттів нітридів, осаджених із застосуванням джерела катодної вакуумно-дугової плазми з фільтром прямолінійного типу. Проаналізовано вплив параметрів імпульсів високовольтного потенціалу зміщення підкладки на швидкість осадження, склад, структуру і механічні властивості покриттів на основі TiN та CrN, у тому числі багатокомпонентних із додаванням Al, Si, Zr ,Y, Re, Nb, Hf. При різних режимах подачі потенціалу забезпечується формування покриттів з нанокристалічною кубічною структурою (типу NaCl) та близьким до стехіометричного вмістом азоту і високою твердістю 25…36 ГПа. З'ясовано, що зміна амплітуди, тривалості та частоти імпульсів дозволяє ефективно керувати морфологією, розміром кристалітів, текстурою, рівнем напружень у покриттях, що впливає на їх механічні властивості. Застосування імпульсного потенціалу зміщення з амплітудою 1…2 кВ, частотою 10…20 кГц та коефіцієнтом заповнення імпульсів 10…15% дає можливість формувати у покриттях різного складу однорідну щільну наноструктуру з текстурою [110] або [100], оптимальним рівнем напружень 4…5 ГПа та гладкою поверхнею. Показано, що така структура забезпечує покращення стійкості покриттів до різних типів зношування. Не виявлено однозначних кореляцій між твердістю покриттів, модулем пружності та їх зносостійкістю.